nature immunology

Intrinsic CD4+ T cell sensitivity and response to a pathogen are set and sustained by avidity for thymic and peripheral complexes of self peptide and MHC

Stephen P Persaud[1], Chelsea R Parker[1], Wan-Lin Lo[1], K Scott Weber[2] & Paul M Allen[1]

Interactions of T cell antigen receptors (TCRs) with complexes of self peptide and major histocompatibility complex (MHC) are crucial to T cell development, but their role in peripheral T cell responses remains unclear. Specific and nonspecific stimulation of LLO56 and LLO118 T cells, which transgenically express a TCR specific for the same *Listeria monocytogenes* epitope, elicited distinct interleukin 2 (IL-2) and phosphorylated kinase Erk responses, the strength of which was set in the thymus and maintained in the periphery in proportion to the avidity of the binding of the TCR to the self peptide–MHC complex. Deprivation of self peptide–MHC substantially compromised the population expansion of LLO56 T cells in response to *L. monocytogenes in vivo*. Despite their very different self-reactivity, LLO56 T cells and LLO118 T cells bound cognate peptide–MHC with an identical affinity, which challenges associations made between these parameters. Our findings highlight a crucial role for selecting ligands encountered during thymic 'education' in determining the intrinsic functionality of CD4+ T cells.

The initiation of CD4+ T cell responses requires productive interactions between the T cell antigen receptor (TCR) and complexes of peptide and major histocompatibility complex (MHC) class II[1,2]. Such interactions are highly sensitive and specific despite having binding affinities in the micromolar range[3]. Even weaker interactions between the TCR and complexes of self peptide and MHC (self peptide–MHC) serve critical roles in the development, survival and peripheral function of T cells[4–8]. It is evident that the TCR can discriminate between peptide-MHC ligands, even subtly different ones[9], to signal distinct functional outcomes. It remains an important pursuit to understand the molecular features of interactions between the TCR and peptide-MHC complexes that promote effective CD4+ T cell responses to pathogens.

The affinity of the TCR for cognate peptide–MHC and clonal frequency in the preimmune repertoire are important factors that govern the magnitude of the *in vivo* responses of CD4+ or CD8+ T cells to pathogens[10–14]. CD4+ or CD8+ T cells of higher affinity with greater functional avidity for antigen are more prevalent after infection than before, which demonstrates evolution of the antipathogen repertoire. Low-affinity interactions can also lead to the generation of effector and memory CD8+ T cell populations, albeit more slowly and to a lesser extent than that of their counterparts of higher affinity[15].

How the recognition of self peptide–MHC by the TCR affects CD4+ T cell responses has received less attention because of the weak nature of these interactions, the paucity of known endogenous selecting ligands and the difficulty of specifically perturbing self peptide–MHC complexes without also affecting the presentation of cognate antigen. Functionally, the degree of TCR self-reactivity has been correlated with expression of the negative regulator CD5 at the cell surface[16]. The expression of CD5 is set during positive selection in proportion to the strength of signal from self peptide–MHC perceived by the TCR, often referred to as the 'avidity' of the TCR for self peptide–MHC. It has been reported that T cells with greater avidity for self peptide–MHC are more readily positively selected and that this enriches the mature repertoire with clones that bind more strongly to foreign peptide–MHC and respond better to pathogens *in vivo*[17].

To investigate at a clonal level how TCR-peptide-MHC interactions affect CD4+ T cell responses, we used two mouse T cell lines, LLO56 and LLO118. Each line has CD4+ T cells with transgenic expression of a TCR that recognizes an epitope of amino acids 190–205 of the *Listeria monocytogenes* virulence factor listeriolysin O (LLO) bound to the MHC molecule I-A^b. The TCRs were cloned from T cell hybrids generated from C57BL/6 (B6) mice infected with *L. monocytogenes* and thus represent two solutions for recognizing the same pathogen-derived cognate peptide–MHC complex. These cells have a very similar cell surface phenotype, but one notable exception is that LLO56 T cells have much higher expression of CD5 than do LLO118 T cells.

During primary *in vivo* responses to *L. monocytogenes*, LLO118 T cell populations expand more than their LLO56 counterparts do, a response associated with a greater propensity of LLO56 T cells to undergo cell death[18]. Since strong TCR signals can induce cell death during immune responses[19], we set out to determine if on activation, LLO56 T cells perceive such strong TCR signals as to induce the substantial cell death observed before. We found that not only

[1]Department of Pathology and Immunology, Washington University School of Medicine, St. Louis, Missouri, USA. [2]Department of Microbiology and Molecular Biology, Brigham Young University, Provo, Utah, USA. Correspondence should be addressed to P.M.A. (pallen@wustl.edu).

Received 13 September 2013; accepted 20 December 2013; published online 2 February 2014; doi:10.1038/ni.2822

did specific stimuli elicit stronger interleukin 2 (IL-2) responses from LLO56 T cells than from LLO118 T cells, but nonspecific stimuli that bypassed the TCR also produced the same result, which suggested intrinsic differences in the responsiveness of the two T cell lines to stimulation. The stronger IL-2 responses were associated with more phosphorylation of TCRζ at baseline and of the kinase Erk upon activation. We also found that the basal signaling and responsiveness of LLO56 and LLO118 T cells were not 'hardwired' features of these cells; instead, they were acquired during positive selection in proportion to the avidity of the TCR for selecting self peptide–MHC and required active maintenance by self peptide–MHC in the periphery. Together our data suggest a crucial role for thymic 'education' and TCR self-reactivity in determining the intrinsic functional attributes of $CD4^+$ T cells. Given our observations, we propose a 'TCR-instructive' model whereby selecting TCR–self peptide–MHC interactions establish the function and basal signaling of $CD4^+$ T cells centrally and maintain that functionality in the periphery, ultimately shaping how a given T cell will act during pathogen challenge.

RESULTS

Nonspecific stimuli elicit distinct T cell IL-2 responses

LLO56 and LLO118 T cells showed similar upregulation of expression of the activation markers CD69 and CD25 in response to stimulation with the LLO epitope of amino acids 190–205 (LLO(190–205)) or with antibody to the invariant signaling protein CD3 (anti-CD3) plus antibody to the costimulatory molecule CD28 (anti-CD28) (**Fig. 1a**). That was in accord with our observation that LLO56 and LLO118 T cells proliferated similarly well to antigen *in vitro* and *in vivo* (**Table 1** and **Supplementary Fig. 1a**). However, over the same peptide dose range, LLO56 T cells produced much more IL-2 than did LLO118 T cells (**Fig. 1b**). That result could not be explained by differences in expression of the TCR, CD3, the monomorphic coreceptor CD4 or the costimulatory molecules CD28, CTLA-4, PD-1 or PD-L1 (**Supplementary Fig. 1b**). One possible explanation for it was a difference in affinity of the TCR for the ligand LLO(190–205)–I-A^b. We generated soluble LLO56 and LLO118 TCRs and used surface plasmon resonance (SPR) to assess affinity. The affinity of the LLO56 TCR and LLO118 TCR for LLO(190–205)–I-A^b was identical (**Fig. 1c**), which suggested that the distinct IL-2 responses were not related to differences in binding to LLO–I-A^b. Thus, despite binding cognate antigen with similar affinity and receiving a similarly activating stimulus, LLO56 T cells showed a greater ability to produce IL-2 than did LLO118 T cells.

Stimulation with anti-CD3 plus anti-CD28 also elicited stronger IL-2 response from LLO56 T cells (**Fig. 1b**,**d**). That was also true for cells stimulated with the phorbol ester PMA and ionomycin, which act intracellularly downstream of the TCR (**Fig. 1e**). LLO56 T cells and LLO118 T cells did not differ much in their ability to produce interferon-γ or tumor-necrosis factor in response to PMA and ionomycin (**Fig. 1e**), which indicated that the stronger IL-2 response of LLO56 T cells could not be generalized to all cytokine responses. These findings opposed the presumption that two T cells with different TCRs would respond equally to stimuli that bypass the TCR and suggested that LLO56 T cells and LLO118 T cells bore intrinsic differences that governed the strength of their IL-2 responses, a finding we pursued further, given its potential relevance to the *in vivo* biology of these cells.

Greater Erk and basal TCRζ phosphorylation in LLO56 T cells

To mechanistically understand how nonspecific stimuli could elicit distinct IL-2 responses from LLO56 T cells and LLO118 T cells, we investigated the signaling pathways activated by PMA and ionomycin, including the Ca^{2+}-NFAT, NF-κB and Ras-Erk pathways. Through the use of flow cytometry with phosphorylation-specific antibodies, we found that nonspecific stimulation induced a greater abundance of phosphorylated Erk in LLO56 T cells than in LLO118 T cells (**Fig. 2a**), with similar results obtained by immunoblot analysis (**Supplementary Fig. 2a**). PMA-induced degradation of the inhibitor IκBα (**Fig. 2b**) and ionomycin-induced Ca^{2+} flux (**Fig. 2c**) were similar in LLO56 T cells and LLO118 T cells, with LLO118 T cells showing somewhat stronger responses in each assay. Thus, greater activation of Erk most closely 'tracked' with the stronger IL-2 response to stimulation with PMA and ionomycin in LLO56 T cells.

As stimulation with peptide and antibody also elicited stronger IL-2 responses from LLO56 T cells than from LLO118 T cells, we considered that there might also be differences in proximal signaling. Several studies have linked TCR self-reactivity to the extent of basal TCRζ phosphorylation[17,20,21]. Indeed, we found that LLO56 T cells had a greater basal abundance of p21 (the 21-kilodalton, partially tyrosine-phosphorylated intermediate of the TCRζ) than did LLO118 T cells (**Fig. 2d**). We confirmed the identity of the phosphorylated TCRζ in these experiments with a rabbit antiserum that recognizes both phosphorylated and unphosphorylated TCRζ species (**Supplementary Fig. 2b**). Together these studies demonstrated both basal and inducible differences in cell signaling that were associated with the greater intrinsic IL-2 response of LLO56 T cells.

Strength of the polyclonal T cell response correlates with CD5

Given the differences in the expression of CD5 and basal phosphorylation of TCRζ by LLO56 T cells and LLO118 T cells, we predicted that LLO56 T cells would perceive a stronger TCR signal from self peptide–MHC than would LLO118 T cells. We hypothesized that such a signal might underlie the stronger response of LLO56 T cells to stimulation with PMA and ionomycin. However, to confirm that our observations were not limited only to cells with transgenic expression of a TCR, we sought to determine whether TCR self-reactivity, as gauged by CD5 expression, correlated with the strength of the response to nonspecific stimulation in polyclonal B6 $CD4^+$ or $CD8^+$ T cells, with the prediction that $CD5^{hi}$ T cells (like LLO56 T cells) would be more responsive to stimulation with PMA and ionomycin than $CD5^{lo}$ cells (like LLO118 T cells) would be. We observed that $CD5^{hi}$ $CD4^+$ T cells and $CD5^{hi}$ $CD8^+$ T cells more readily produced IL-2 in response to PMA and ionomycin (**Fig. 3a**) or in response to anti-CD3 plus anti-CD28 (**Supplementary Fig. 3a**) than did their $CD5^{lo}$ counterparts. Stimulation did not substantially alter the distribution of CD5 expression on T cells (**Supplementary Fig. 3b**), a result we confirmed with cells sorted according to their CD5 expression before stimulation (**Supplementary Fig. 3c**). Furthermore, $CD5^{hi}$ $CD4^+$ T cells and $CD5^{hi}$ $CD8^+$ T cells had a greater abundance of phosphorylated Erk after activation and a greater basal abundance of p21 (partially phosphorylated TCRζ) than did their $CD5^{lo}$ counterparts (**Fig. 3b,c**). Because those experiments used bulk $CD4^+$ or $CD8^+$ T cells, which would include memory-phenotype and nonconventional αβ T cells (i.e., regulatory T cells and natural killer T cells), we repeated the analyses with naive conventional αβ T cells ($CD44^{lo}CD25^-NK1.1^-$) sorted by immunomagnetic selection or flow cytometry and obtained identical results (**Fig. 3d–f**). Together these data demonstrated a link among CD5 expression, the intrinsic strength of responses consisting of IL-2 and phosphorylated Erk, and basal signaling in polyclonal T cells, which confirmed the results obtained with LLO56 and LLO118 T cells.

Confirmation that CD5 expression reflects self-reactivity

We sought to confirm the association made between CD5 expression and the self-reactivity of the LLO56 and LLO118 TCRs by an independent assay. Ectopic expression of the human voltage-gated sodium channel (VGSC) subunits SCN4B and SCN5A gives AND T cells (which have transgenic expression of a TCR specific for moth cytochrome *c*) the ability to respond to the self peptide gp250 in complex with the MHC molecule I-E^k (their endogenous selecting ligand)[22]. We reasoned that such a gain-of-function approach could be extended to gauge the self-reactivity of T cells with unknown selecting ligands. For this, we transfected LLO56 T cells, LLO118 T cells and B6 $CD4^+$ T cells to express SCN4B linked to the fluorescent marker mCherry and SCN5A linked to green fluorescent protein constructs (i.e., the VGSC), then cultured the cells with or without irradiated B6 antigen-presenting cells (APCs) and then analyzed their activation by upregulation of CD69 expression. We identified $VGSC^+$ cells as those that coexpressed the fluorescent markers from each construct. We unequivocally identified LLO56, LLO118 and B6 $CD4^+$ T cells from cultures on the basis of expression of the TCRα variable region $V_\alpha 2$ (used by the LLO56 and LLO118 TCRs), along with expression of the unique congenic markers Thy-1.1 (CD90.1) and Ly5.1 (CD45.1) (expressed by LLO56 T cells and LLO118 T cells, respectively) (**Supplementary Fig. 4a**).

After culture with B6 APCs, $VGSC^+$ LLO56 T cells showed greater upregulation of CD69 expression than did $VGSC^+$ LLO118 T cells, as would be predicted given their respective CD5 expression (**Supplementary Fig. 4b**). $VGSC^+$ B6 $CD4^+$ T cells, whose mean CD5 expression was between that of LLO56 T cells and that of LLO118 T cells (**Supplementary Fig. 1b**), showed intermediate upregulation of CD69 expression (**Supplementary Fig. 4b**). $VGSC^+$ B6 T cells, LLO56 T cells and LLO118 T cells showed equivalent upregulation of CD69 expression when cultured with B6 APCs pretreated with anti-I-A^b (**Supplementary Fig. 4b**). The blockade with anti-I-A^b did not reduce the response to APCs to the baseline response of control

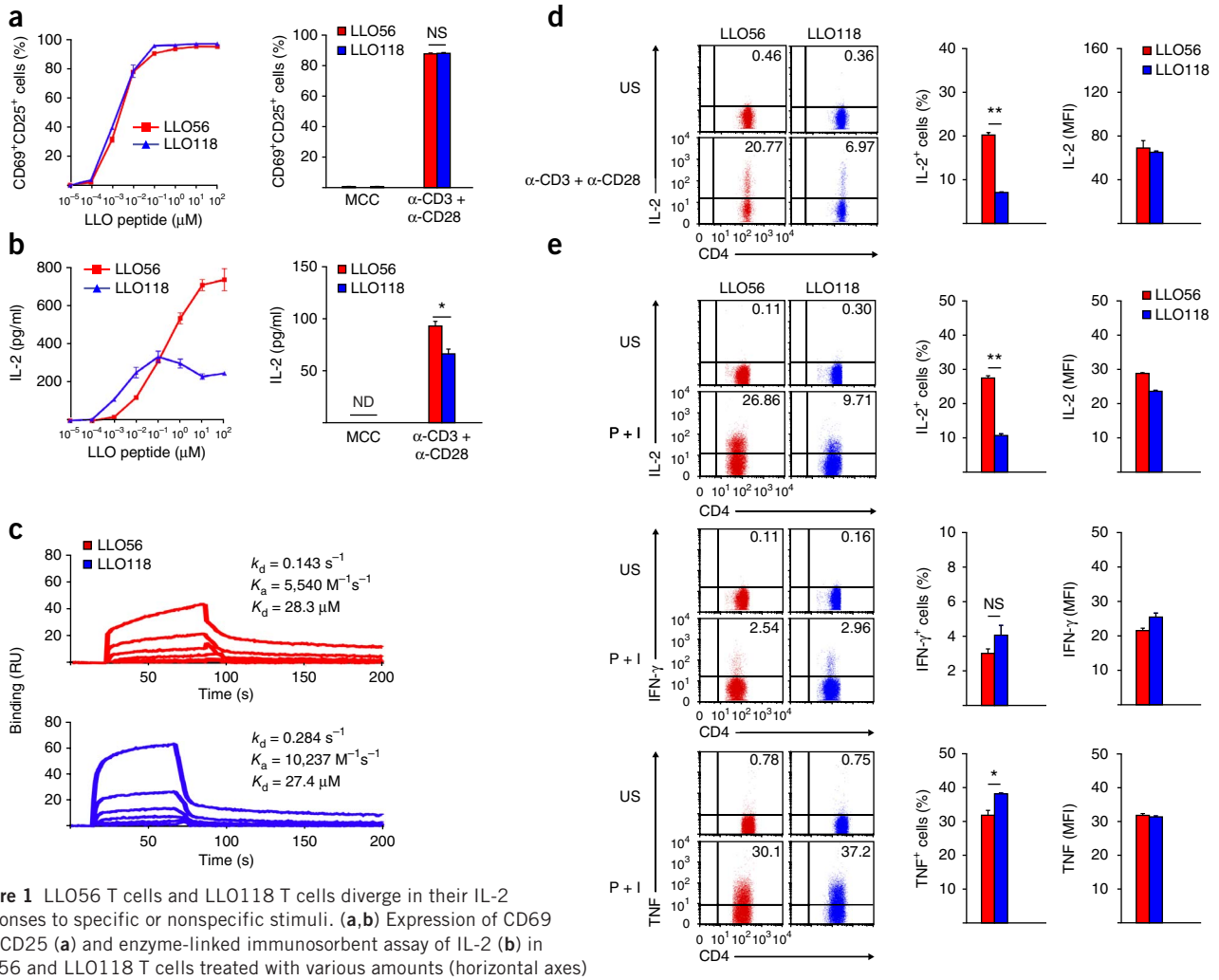

Figure 1 LLO56 T cells and LLO118 T cells diverge in their IL-2 responses to specific or nonspecific stimuli. (**a**,**b**) Expression of CD69 and CD25 (**a**) and enzyme-linked immunosorbent assay of IL-2 (**b**) in LLO56 and LLO118 T cells treated with various amounts (horizontal axes) of LLO(190–205) (left) or 100 μM of moth cytochrome *c* amino acids 83–101 (MCC) or anti-CD3 and anti-CD28 (α-CD3 + α-CD28; 10 μg/ml each). ND, not detectable. (**c**) Binding of LLO56 and LLO118 TCRs to LLO(190–205)–I-A^b, assessed as surface plasmon resonance of a series of concentrations of single-chain TCRs (40 μM (top curves), followed by twofold serial dilutions (top to bottom)), presented as response units (RU) and as the dissociation rate constant (k_d), association rate constant (K_a) and dissociation constant (K_d). (**d**) IL-2-capture assay of LLO56 and LLO118 $CD4^+$ T cells left unstimulated (US) or stimulated with anti-CD3 plus anti-CD28 (10 μg/ml), assessed by flow cytometry (left) and presented as frequency of $IL\text{-}2^+$ $CD4^+$ cells (middle) and mean fluorescence intensity (MFI) of IL-2 in $CD4^+$ cells (right). (**e**) Intracellular IL-2, interferon-γ (IFN-γ) and tumor-necrosis factor (TNF) in LLO56 and LLO118 $CD4^+$ T cells left unstimulated (US) or stimulated with PMA and ionomycin (P + I), presented as in **d**. Numbers in quadrants (**d**,**e**) indicate percent cytokine-positive $CD4^+$ cells. NS, not significant; $^*P < 0.05$ and $^{**}P < 0.0001$ (unpaired two-tailed Student's *t* test). Data are representative of at least three experiments (mean and s.e.m. in **a**,**b**,**d**,**e**).

Table 1 Responses of LLO56 and LLO118 T cells to antigen

Parameter	LLO56	LLO118
Primary expansion in response to *Listeria in vivo*	+	+++
Proliferation in response to LLO(190–205) or to *Listeria in vitro*	+	+
Proliferation during primary response to *Listeria in vivo*	+	+
Cell death during primary response to *Listeria in vivo*	+++	+

Characteristics of the responses of LLO56 and LLO118 T cells to *L. monocytogenes* antigen *in vitro* and *in vivo*, as identified before[18].

cells not exposed to APCs (**Supplementary Fig. 4b**), which suggested either incomplete blockade of MHC class II or unanticipated reactivity to other self molecules that was similar for all groups. We did not observe upregulation of CD69 expression in untransfected cells or cells transfected to express SCN4B-mCherry alone, for cells cultured with B6 APCs (**Supplementary Fig. 4b**). Furthermore, the extent of upregulation of CD69 expression by VGSC$^+$ T cells cultured with B6 APCs did not correlate with expression of the channel subunits SCN4B and SCN5A (**Supplementary Fig. 4c**). These results provided additional support for our conclusion that the CD5^{hi} LLO56 T cells reacted more strongly to self peptide–MHC than did CD5^{lo} LLO118 T cells.

Strength of intrinsic T cell response set by thymic selection

Because T cell development is predicated on TCR interactions with self peptide–MHC, we reasoned that analysis of thymic selection would yield insights into the origin of the biology of LLO56 and LLO118 T cells. LLO56 thymi had a much higher frequency and number of CD4$^+$ single-positive (CD4SP) thymocytes than did LLO118 thymi (**Fig. 4a**) but had fewer total thymocytes (**Fig. 4a**). Together with the considerably larger population of TCR^{hi}CD69$^+$ post-selection thymocytes (**Supplementary Fig. 5a**), this observation suggested that LLO56 CD4$^+$CD8$^+$ double-positive (DP) thymocytes were more efficiently positively selected than were their LLO118 counterparts. Consistent with that, post-selection LLO56 thymocytes had higher expression of CD5 and CD69, two markers whose expression was upregulated in response to the strength of the selecting signal (**Fig. 4b**). The finding that LLO118 T cells received a weaker signal from self peptide–MHC than did LLO56 T cells suggested that the lower frequency of LLO118 CD4SP thymocytes was not due to negative selection.

To investigate whether positively selecting interactions of the TCR with self peptide–MHC in the thymus determined the intrinsic IL-2 responses of LLO56 and LLO118 T cells, we stimulated LLO56 and LLO118 thymocytes with PMA and ionomycin and analyzed their IL-2 production at each developmental stage. We detected similarly high frequencies of IL-2-producing cells among LLO56 and LLO118 CD4$^-$CD8$^-$ (double-negative) thymocytes (**Fig. 4c**). Any contribution from natural killer cells, natural killer T cells or γδ T cells to this IL-2 response was negligible, given their low frequencies (**Supplementary Fig. 5b**). LLO56 and LLO118 DP thymocytes were similarly refractory to stimulation with PMA and ionomycin (**Fig. 4c**). However, as DP thymocytes transitioned to the CD4SP stage, we observed that a higher frequency of LLO56 CD4SP thymocytes than LLO118 CD4SP thymocytes produced IL-2, and LLO56 CD4SP thymocytes had more Erk phosphorylation and basal p21 (partial TCRζ phosphorylation) than did their LLO118 counterparts (**Fig. 4c–e** and **Supplementary Fig. 5c**), which reproduced the difference noted in mature LLO56 T cells and LLO118 T cells.

To further assess the proposal that the selecting MHC environment affects the intrinsic IL-2 responses of mature CD4$^+$ T cells, we took advantage of the fact that AND T cells are selected strongly in H-2^k mice and more weakly in H-2^b mice[23]. That allowed us to investigate whether differences in intrinsic functionality were detectable in T cells that expressed the same TCR but that had developed on different MHC backgrounds. Indeed, AND T cells selected on H-2^k MHC had much stronger intrinsic IL-2 responses than those of cells selected on H-2^b MHC (**Supplementary Fig. 5d**). Together with the data obtained with LLO56 and LLO118 mice, our results demonstrated that intrinsic T cell responsiveness was set during T cell development in proportion to the strength of the selecting signals from self peptide–MHC.

Finally, we considered that if stronger TCR signaling in LLO56 T cells predisposed them to TCR-driven cell death *in vivo*, a greater propensity to undergo cell death might be evident in post-selection LLO56 T cells, having emerged alongside its greater basal TCR signaling. We tested that idea by stimulating LLO56 and LLO118 thymocytes and peripheral T cells with anti-CD3 plus anti-CD28 in culture. While preselection LLO118 thymocytes showed greater cell death than did their LLO56 counterparts, that pattern reversed in post-selection thymocytes and peripheral T cells (**Fig. 4f**). The cell-death responses of pre- and post-selection LLO56 and LLO118 thymocytes were associated with basal phosphorylation of TCRζ, with a higher average per-cell abundance of p21 (partially phosphorylated TCRζ) seen when greater cell death was observed (**Fig. 4e**). Differences in expression of the IL-7 receptor chain IL-7Rα and the antiapoptotic molecule Bcl-2 could not explain the differences between LLO56 cells and LLO118 cells in their cell-death activity during T cell development (**Supplementary Fig. 5e**). While expression of the proapoptotic Bcl-2 family member Bim was higher in LLO56 CD4SP thymocytes

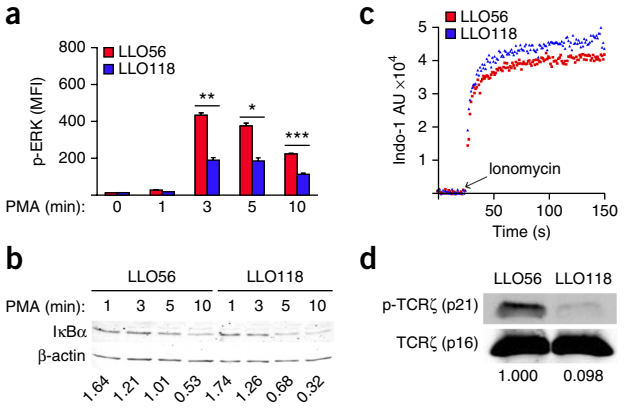

Figure 2 The stronger IL-2 responses of LLO56 T cells are linked to greater activation-induced phosphorylation of Erk and basal phosphorylation of TCRζ than that of LLO118 T cells. (**a**) Kinetics of Erk phosphorylation in LLO56 and LLO118 T cells stimulated for 0–10 min with PMA (horizontal axis). $^*P < 0.01$, $^{**}P < 0.001$ and $^{***}P < 0.0001$ (unpaired two-tailed Student's *t*-test). (**b**) Kinetics of the degradation of IκBα and β-actin (control) in LLO56 and LLO118 T cells stimulated for 0–10 min with PMA (above lanes); numbers below lanes indicate IκBα band density relative to that of β-actin (IκBα/β-actin). (**c**) Ca^{2+} flux of ionomycin-treated LLO56 and LLO118 T cells, assessed by flow cytometry with one measurement per second and presented (in arbitrary units (AU)) as fluorescence of the Ca^{2+} indicator dye Indo-1 (violet/blue). (**d**) Basal phosphorylation of TCRζ (p21) and total basal TCRζ (p16) in whole-cell lysates of unstimulated LLO56 and LLO118 T cells; numbers below lanes indicate p21 band density normalized to that of p16 and presented relative to that of LLO56 cells. Data are representative of at least three independent experiments (mean and s.e.m. in **a**).

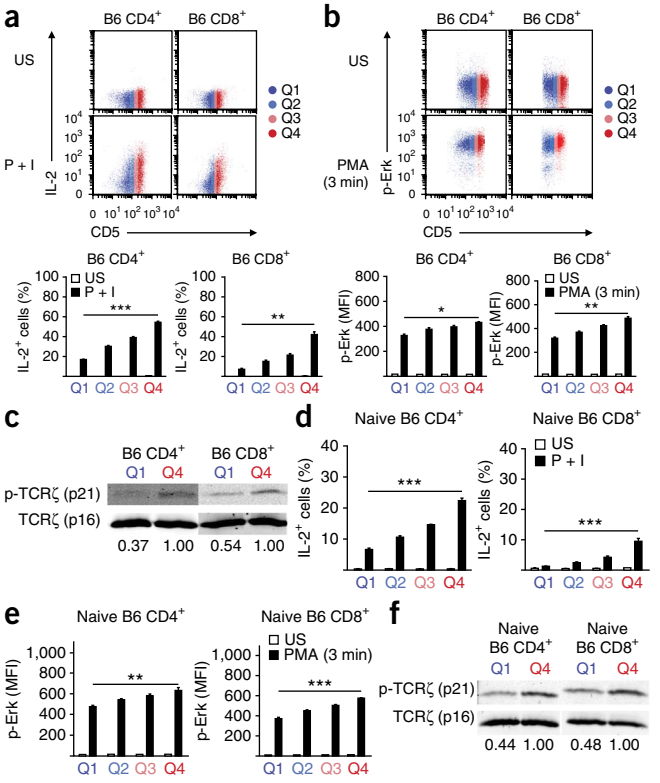

Figure 3 Strength of intrinsic IL-2 responses and signaling in polyclonal B6 CD4$^+$ and CD8$^+$ T cells correlates with CD5 expression. (**a**,**b**) IL-2 production (**a**) and phosphorylated (p-) Erk (**b**) in B6 CD4$^+$ T cells (left) and CD8$^+$ T cells (right) left unstimulated or stimulated with PMA and ionomycin (**a**) or stimulated for 3 min with PMA (**b**), gated into four equal fractions (Q1–Q4) from lowest to highest CD5 expression (top). Below, frequency of IL-2$^+$ cells (**a**) and mean fluorescence intensity of phosphorylated Erk (**b**) for the cells above. (**c**) Basal TCRζ phosphorylation and total TCRζ (as in **Fig. 2d**) in whole-cell lysates of unstimulated B6 CD4$^+$ and CD8$^+$ T cells sorted by flow cytometry from the Q1 and Q4 fractions in **a**,**b**; numbers below lanes indicate p21 band density normalized to that of p16 and presented relative to that of the Q4 fraction. (**d**–**f**) IL-2 production (**d**), Erk phosphorylation (**e**) and basal TCRζ phosphorylation (**f**) in sorted naive conventional (CD44$^{lo–int}$CD25$^-$NK1.1$^-$) CD4$^+$ and CD8$^+$ T cells (presented as in **a**–**c**). $^*P < 0.01$, $^{**}P < 0.001$ and $^{***}P < 0.0001$ (unpaired two-tailed Student's *t*-test). Data are representative of at least three independent experiments (mean and s.e.m. in **a**,**b**,**d**,**e**).

than in their LLO118 counterparts, this difference did not persist in peripheral cells (**Supplementary Fig. 5e**), which would make it an unlikely contributor to the greater cell death observed in that setting. Thus, the greater propensity of LLO56 T cells than LLO118 T cells to undergo cell death paralleled the emergence of greater basal TCR signaling in LLO56 T cells. The finding that cells experiencing stronger TCR signals were more susceptible to cell death was in agreement with published work[19].

Self peptide–MHC maintains intrinsic responses of mature T cells

After leaving the thymus, T cells continue to receive tonic self peptide–MHC signals in the periphery. We next assessed whether deprivation of self peptide–MHC compromised CD4$^+$ T cell responses beyond the most proximal TCR signaling components. For this, we analyzed the IL-2 responses of LLO56 and LLO118 T cells to PMA and ionomycin *ex vivo* 4 d after adoptive transfer of the cells into B6 or MHC class II–deficient recipient mice. Cells transferred into MHC class II–deficient mice had expression of CD3, CD4 or TCRs similar to that of cells transferred into B6 mice, but they did have lower expression of CD5 (**Supplementary Fig. 6a**), as might be expected for a molecule dynamically regulated by TCR–self peptide–MHC signals[24,25].

After transfer into B6 mice, LLO56 T cells showed stronger IL-2 responses to PMA and ionomycin than those of their LLO118 counterparts (**Fig. 5a**), as observed with freshly isolated cells. However, transfer into MHC class II–deficient mice rendered both LLO56 T cells and LLO118 T cells poorly responsive to PMA and ionomycin (**Fig. 5a**). To exclude the possibility that the absence of CD4$^+$ T cells in MHC class II–deficient recipients contributed to the diminished IL-2 responses, we analyzed the IL-2 responses of LLO56 and LLO118 T cells transferred into two additional sets of recipients: mice deficient in the α-chain constant region of the TCR (which have normal MHC class II but lack αβ T cells) and H-2M-deficient mice (which have αβ T cells but whose repertoire of MHC class II–bound self peptides is largely restricted to the invariant chain–derived peptide CLIP). The goal of these additional transfer experiments was to determine whether self peptide–MHC or bystander αβ T cells regulated the intrinsic IL-2 responses of LLO56 and LLO118 T cells.

At 4 d after being transferred into recipients deficient in the α-chain constant region of the TCR, LLO56 T cells showed greater IL-2 production than did their LLO118 counterparts in response to PMA and ionomycin, as observed for freshly isolated cells and cells transferred into B6 mice (**Supplementary Fig. 6b**). However, transfer into H-2M-deficient mice rendered both LLO56 T cells and LLO118 T cells poorly responsive to stimulation, as observed after transfer into MHC class II–deficient mice (**Supplementary Fig. 6b**). These results indicated that the intrinsic strength of the IL-2 responses of LLO56 and LLO118 T cells was actively maintained by TCR–self peptide–MHC interactions.

We next assessed the kinetics of the loss of intrinsic IL-2 responses upon withdrawal of self peptide–MHC. We focused on LLO56 T cells for these experiments, as the large dynamic range of IL-2 responses of LLO56 T cells deprived of MHC class II and those not deprived of MHC class II was most appropriate for the resolution of changes in IL-2 responses over time. We transferred LLO56 T cells into H-2M-deficient mice and then, 1, 2 and 4 d later, purified the cells and activated them with PMA and ionomycin. LLO56 T cells deprived of self peptide–MHC for 1 d showed a sharp decrease in their IL-2 response to PMA and ionomycin, with a more subtle decrease thereafter, relative to the response of freshly isolated LLO56 T cells (**Supplementary Fig. 6c**). Thus, intrinsic IL-2 responses decayed rapidly in the absence of self peptide–MHC ligands.

We next sought to determine whether deprivation of self peptide–MHC ligands affected the activation of Erk. LLO56 T cells transferred into MHC class II–deficient recipients showed less phosphorylation of Erk than did LLO56 T cells transferred into B6 mice (**Fig. 5b**). We obtained the same result for LLO118 T cells transferred into MHC class II–deficient and B6 mice, although the lower Erk phosphorylation after the loss of MHC class II was more modest for LLO118 T cells than for LLO56 T cells (**Fig. 5b**). These experiments provided evidence that the signal from self peptide–MHC affected TCR signaling as far downstream as Erk.

Finally, we investigated whether deprivation of self peptide–MHC signals affected the responses of LLO56 and LLO118 T cells to *L. monocytogenes in vivo*. For this, we transferred LLO56 or LLO118 T cells into MHC class II–deficient or B6 mice and thus generated

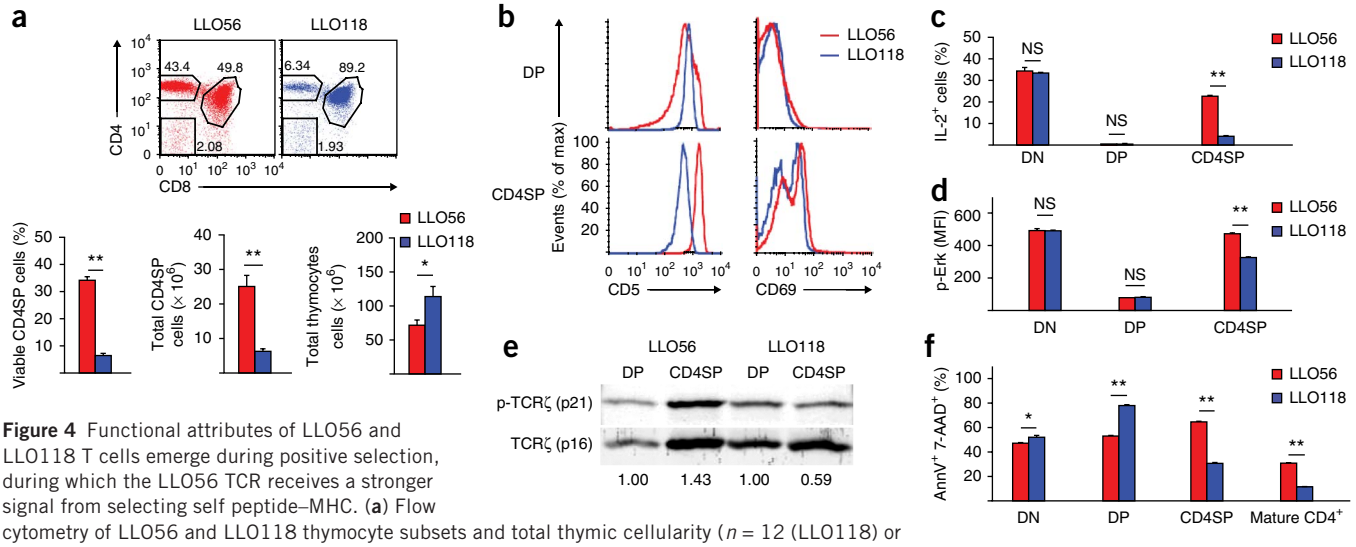

Figure 4 Functional attributes of LLO56 and LLO118 T cells emerge during positive selection, during which the LLO56 TCR receives a stronger signal from selecting self peptide–MHC. (**a**) Flow cytometry of LLO56 and LLO118 thymocyte subsets and total thymic cellularity ($n = 12$ (LLO118) or 13 (LLO56) thymuses). Numbers adjacent to outlined areas indicate percent cells in each. (**b**) Expression of markers reflecting avidity for self peptide–MHC in DP (pre-selection) and CD4SP (post-selection) thymocytes from LLO56 or LLO118 thymuses ($n \geq 3$ each). (**c**,**d**) Intracellular IL-2 (**c**) and Erk phosphorylation (**d**) in LLO56 and LLO118 thymocytes stimulated with PMA and ionomycin (**c**) or stimulated for 3 min with PMA (**d**), gated and analyzed by subset. (**e**) Basal TCRζ phosphorylation and total TCRζ (as in **Fig. 2d**) in unstimulated DP and CD4SP thymocytes sorted by flow cytometry from LLO56 and LLO118 mice (1.7×10^6 cells per lane); numbers below lanes indicate p21 band density normalized to that of p16 and presented relative to that of DP thymocytes. (**f**) Frequency of dead (annexin V–positive (AnnV$^+$) and 7-AAD$^+$) cells among LLO56 and LLO118 thymocytes of various subsets and peripheral CD4$^+$ T cells stimulated for 24 h with anti-CD3 and anti-CD28 (1 μg/ml each) and stained with annexin V and the DNA-intercalating dye 7-AAD. $^*P < 0.05$ and $^{**}P < 0.0001$ (unpaired two-tailed Student's *t*-test). Data are representative of at least six experiments (**a**,**b**), at least three experiments (**c**,**d**), five experiments (**e**) or four experiments (**f**; mean and s.e.m. in **a**,**c**,**d**,**f**).

pools of cells that were deprived of MHC class II or not. We then transferred those cells into cohorts of B6 mice that had been infected with *L. monocytogenes* the previous day. We timed the adoptive transfers so that T cells were introduced into the infected mice at 1.5 d after infection, at which point the presentation of *L. monocytogenes* antigens is abundant in the spleen[26]. The intravenously transferred LLO56 or LLO118 T cells would home to the spleen first, promoting rapid encounter with LLO–I-A^b complexes. We then assessed the overall population expansion of the transferred cells at day 7 after transfer (**Supplementary Fig. 6d**). The goal of this system was to encourage the transferred cells to undergo activation before they had a chance to regain tonic signaling from the self peptide–MHC normally present in B6 mice.

LLO56 T cells deprived of MHC class II expanded considerably less than did LLO56 T cells that were not deprived of MHC class II at day 7 after transfer into *L. monocytogenes*–infected B6 mice (**Fig. 5c**). The responses of LLO118 T cells at day 7 after transfer were similarly strong whether the cells were deprived of self peptide–MHC or not (**Fig. 5c**). These data demonstrated that deprivation of TCR–self peptide–MHC interactions affected the responses of CD4$^+$ T cells to pathogen *in vivo*; the common theme in this and our other experiments involving withdrawal of self peptide–MHC was that LLO56 T cells, which receive stronger tonic signaling from self peptide–MHC than did LLO118 T cells, showed greater functional deficits when deprived of such signals.

CD5 feedback inhibition of T cell self-reactivity

It remains unclear whether CD5 itself influences the intrinsic strength of IL-2 responses or is merely a marker for TCR–self peptide–MHC avidity. The literature has provided conflicting data about whether CD5 augments or interferes with TCR signaling and in which contexts it does so[16,27–29]. To address this issue, we generated LLO56 and LLO118 mice deficient in CD5. CD5-deficient LLO56 thymocytes perceived a stronger signal from self peptide–MHC than

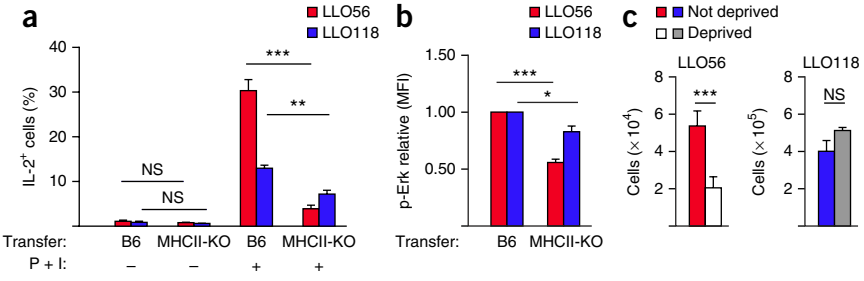

Figure 5 Deprivation of self peptide–MHC compromises intrinsic IL-2 and Erk responses and *in vivo* responses to *L. monocytogenes*. (**a**) IL-2 responses of LLO56 and LLO118 T cells transferred into B6 mice ($n = 6$ (LLO56) or 7 (LLO118)) or MHC II–deficient mice (MHCII-KO; $n = 8$ (LLO56) or 6 (LLO118)), then collected 4 d after transfer and left unstimulated (–) or stimulated (+) *ex vivo* with PMA and ionomycin, presented as the frequency of IL-2$^+$ cells. (**b**) Phosphorylation of Erk in LLO56 and LLO118 T cells transferred into B6 mice ($n = 7$ (LLO56) or 6 (LLO118)) or MHC II–deficient mice (MHCII-KO; $n = 5$ (LLO56) or 5 (LLO118)), then collected 4 d after transfer and stimulated *ex vivo* for 3 min with PMA, presented as the mean fluorescence intensity of cells transferred into MHC II–deficient recipients relative to that of cells transferred into B6 recipients in the same experiment. (**c**) Population expansion of LLO56 and LLO118 T cells deprived of self peptide–MHC ($n = 12$ (LLO56) or 6 (LLO118) recipient mice) or not ($n = 12$ (LLO56) or 7 (LLO118) recipient mice) at 7 d after transfer into *L. monocytogenes*–infected B6 mice. $^*P < 0.05$, $^{**}P < 0.001$ and $^{***}P < 0.0001$ (unpaired (**a**,**b**) or paired (**c**) two-tailed Student's *t*-test). Data are pooled from three experiments (**a**), three or four experiments (**b**), six experiments (**c**, LLO56) or four experiments (**c**, LLO118; mean and s.e.m.).

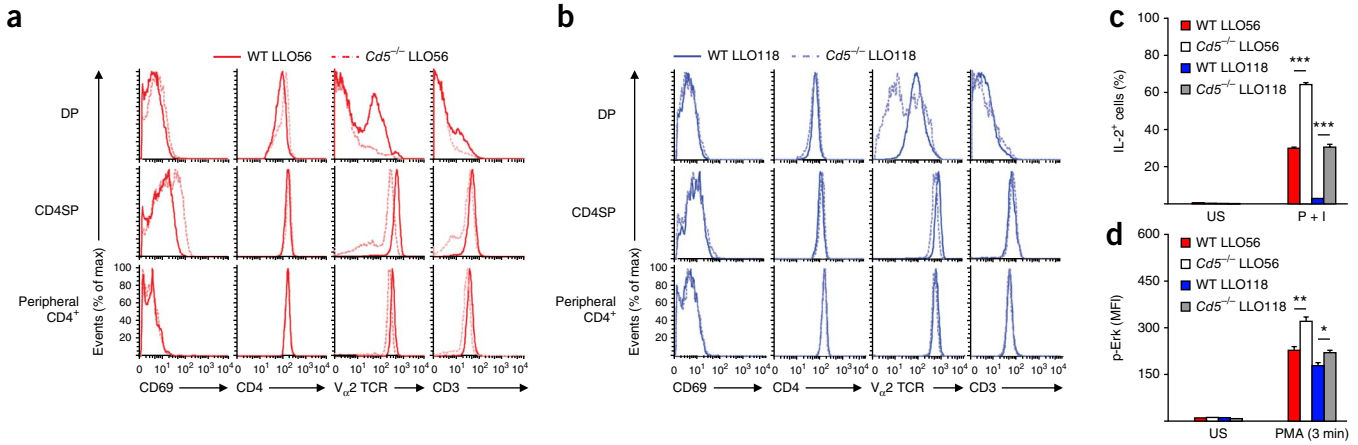

Figure 6 CD5 antagonizes signaling from self peptide–MHC and intrinsic IL-2 and phosphorylated Erk responses. (**a**,**b**) Expression of functional markers (horizontal axes) in wild-type (WT) and CD5-deficient (*Cd5*$^{-/-}$) LLO56 (**a**) and LLO118 (**b**) thymocyte subsets and peripheral cells. (**c**,**d**) Intracellular IL-2 (**c**) and Erk phosphorylation (**d**) in wild-type and CD5-deficient LLO56 and LLO118 thymocytes left unstimulated or stimulated with PMA and ionomycin (**c**) or stimulated for 3 min with PMA (**d**) (presented as in **Fig. 4c**,**d**). $*P < 0.05$, $**P < 0.01$ and $***P < 0.0001$ (unpaired two-tailed Student's *t* test). Data are representative of two (LLO118) or three (LLO56) experiments (mean and s.e.m. in **c**,**d**).

did wild-type LLO56 thymocytes, as judged by their higher CD69 expression at the CD4SP stage (**Fig. 6a**). The greater self-reactivity of CD5-deficient LLO56 cells might have been offset by compensatory reductions in expression of the TCR and CD3 in post-selection cells. Conversely, CD5-deficient LLO118 thymocytes did not show higher CD69 expression after selection than did their wild-type LLO118 counterparts, and peripheral CD5-deficient LLO118 T cells did not show reduced surface expression of TCR or CD3 (**Fig. 6b**).

CD5-deficient LLO56 and LLO118 T cells had much higher intrinsic IL-2 responses to stimulation with PMA and ionomycin than did their wild-type counterparts (**Fig. 6c**), a result associated with moderate increases in PMA-induced Erk signaling (**Fig. 6d**). These findings supported the view that CD5 antagonized self peptide–MHC signals from the TCR, reducing the intrinsic IL-2 responsiveness maintained by TCR–self peptide–MHC interactions, which effectively ruled out the possibility that the reduction in CD5 expression seen in the MHC class II–deprivation experiments caused the observed reduction in responses involving IL-2 and phosphorylated Erk. The finding that the cells with the strongest IL-2 responses had the highest CD5 expression suggested that CD5 does not impose a dominant inhibitory tone. Instead, since CD5 expression was set and maintained on the basis of the strength of TCR–self peptide–MHC interactions, CD5 is positioned to impose feedback inhibition on TCR signaling to restrain the most strongly self-reactive cells[30].

DISCUSSION

There has been great interest in understanding the factors that determine the fate and function of developing T cells in the thymus. For conventional αβ T cells, invariant natural killer T cells and regulatory T cells[31–33], considerable evidence has demonstrated that the interaction of TCRs with self ligands provides essential instructive signals that drive maturation into these lineages. Indeed, what the TCR 'sees' can guide an uncommitted thymocyte toward one of a variety of cell types with disparate effector functions. This raises the issue of how the recognition of self ligands by TCRs induces distinct developmental signals that lead to such profoundly different fates.

In this study, we demonstrated unanticipated intrinsic differences in the IL-2 responses of the pathogen-responsive LLO56 and LLO118 T cells that originated and were actively maintained by the avidity of the TCR for self peptide–MHC. The basis for how the recognition of self peptide–MHC molecules by TCRs gives rise to different intrinsic responsiveness remains elusive. In the absence of known selecting ligands, it is difficult to speculate about whether binding strength or ligand availability affects the self-reactivity of LLO56 and LLO118 TCRs, or whether the TCRs recognize the same or different self ligands. If TCRs bind self peptide–MHC and cognate peptide–MHC with a similar docking orientation, it is plausible that the highly dissimilar CDR3β regions of the LLO56 and LLO118 TCRs could mediate different interactions with self peptides.

Signals derived from the ligation of self peptide–MHC complexes by TCRs have generally been studied through the use of surrogate markers such as CD5 or by the analysis of basal activation of proximal TCR signaling pathway components such as TCRζ[17,20,21]. The effect of self peptide–MHC on signaling further downstream of the TCR has received less attention, but such an effect might be expected, given the many aforementioned functions of TCR–self peptide–MHC interactions[4–8]. B cells receiving a stronger signaling from endogenous antigen produce stronger calcium responses upon stimulation, but a similar result has not been observed for T cells, mirroring the results of our own calcium-flux experiments[34]. Using PMA to elicit responses far downstream of the TCR, we directly linked the strength of phosphorylated Erk responses with the avidity of the TCR–self peptide–MHC interaction. Thus, the ligation of self peptide–MHC complexes by TCRs affected the signaling of mature T cells to such an extent that even stimulation with PMA was unable to bypass its influence. A mechanistic possibility for this is drawn from the demonstration that strong selecting signals from self peptide–MHC complexes promote the localizion of Erk to the plasma membrane[35]. Applying that concept to our system, stronger signals from self peptide–MHC complexes in peripheral LLO56 T cells could better facilitate the assembly of signaling components at the plasma membrane[21] and thus coordinate and strengthen the activation of Erk.

Our study has provided evidence that deprivation of self peptide–MHC affected a CD4$^+$ T cell response to infection *in vivo*. However, if propensity to cell death 'tracked with' stronger basal signaling, withdrawal of self peptide–MHC might then be expected to mitigate the amount of cell death seen and lead to improved rather than abrogated *in vivo* population expansion of LLO56 T cells. The finding that LLO56 T cell populations nevertheless expanded to a lesser

extent than LLO118 T cells did suggested that the same cell death–driven differences in population expansion were manifest in the self peptide–MHC–withdrawal model and in the original adoptive-transfer model[18]. It is possible that even if the basal signaling and cell-death activity of LLO56 T cells were to be 'reset' by an initial withdrawal of MHC class II, those signaling and death characteristics could eventually rebound upon reexposure to self peptide–MHC in B6 mice over the duration of the experiment.

Finally, a published report has concluded that the self-reactivity of CD4$^+$ T cells correlates with affinity for cognate peptide–MHC and efficacy in responding to pathogen[17]. Our studies of LLO56 and LLO118 T cells, which differ considerably in their self-reactivity yet have identical affinity for LLO–I-A^b, challenge the generality of correlations between reactivity to self peptide–MHC and reactivity to foreign peptide–MHC. It is plausible that if selection favors TCRs able to recognize general structural features of peptide-MHC complexes, the resulting repertoire would show enrichment for TCRs that might bind more strongly to any particular peptide-MHC complex. However, the repertoire is nevertheless anticipatory in terms of the wide variety of foreign peptides that might be encountered. There is no direct selective pressure that dictates that the handful of TCRs able to bind a specific set of pathogen-derived epitopes must have a particular avidity for self peptide–MHC beyond that necessary to get the cell through selection. Thus, as demonstrated by LLO56 and LLO118 T cells, we would expect that T cells with sufficient affinity for foreign peptide–MHC could be found across the spectrum of CD5 expression.

Several reports have also suggested that greater avidity of the TCR for cognate peptide–MHC or self peptide–MHC is not necessarily a property of effective *in vivo* responses. After infection with lymphocytic choriomeningitis virus or the induction of experimental autoimmune encephalitis, most CD4$^+$ T cells were shown to have undetectable binding to peptide–I-A^b tetramers loaded with the epitope of lymphocytic choriomeningitis virus glycoprotein amino acids 61–80 (foreign antigen) or the epitope of myelin oligodendrocyte glycoprotein amino acids 35–55 (self antigen); however, a high frequency of those tetramer-negative cells achieved detectable, specific binding when assessed by kinetic measurement of *in situ* binding[36,37]. Those low-affinity glycoprotein-specific T cells were substantial contributors of effector cytokines during primary infection with lymphocytic choriomeningitis virus or experimental autoimmune encephalitis, which challenges the premise that the T cells expressing TCRs with the highest affinity for foreign peptide–MHC or self peptide–MHC dominate immune responses. Two studies have demonstrated that the duration of TCR–cognate peptide–MHC interactions, rather than overall affinity, is the most predictive parameter of the effector differentiation[38] and memory differentiation[39] of CD4$^+$ T cells. Finally, Ly6C$^-$ CD4$^+$ T cell populations show enrichment for CD5^{hi} cells that 'preferentially' develop into induced regulatory T cells during immune responses and exhibit poorer *in vivo* population expansion than that of their Ly6C^{hi} CD5^{lo} counterparts[40]. Those studies and our results here demonstrate the complexity of which properties of TCR–peptide–MHC interactions generate more effective CD4$^+$ T cells responses, a complexity that is not accounted for by a model that correlates the binding of foreign peptide–MHC and self peptide–MHC by TCRs to the magnitude of the response.

Indeed, the quality of CD4$^+$ T cell responses involves the interplay of many contributing factors. Our work has emphasized the importance of TCR–self peptide–MHC interactions in determining the inherent responsiveness to stimulation and basal signaling in T cells, with implications for the performance of CD4$^+$ T cells *in vivo*. We conclude that thymic 'education' is a critical inflection point about which these intrinsic functional attributes are determined.

METHODS

Methods and any associated references are available in the online version of the paper.

Note: Any Supplementary Information and Source Data files are available in the online version of the paper.

ACKNOWLEDGMENTS

We thank E. Huseby (University of Massachusetts Medical School) for soluble I-A^b; Q.J. Li for generating the LLO56 and LLO118 TCR-encoding transgene constructs; J. Ting (University of North Carolina Chapel Hill School of Medicine) for mice doubly deficient in H-2M and β_2-microglobulin; K. Murray (Vanderbilt University School of Medicine) for the SCN5A–green fluorescent protein construct; D. Kreamalmeyer for mouse breeding and care; S. Horvath for peptide synthesis; D. Brinja and E. Lantelme for assistance with sorting by flow cytometry; D. Donermeyer, A. Shaw, E. Unanue and E. Brown for comments on the manuscript; and A. Chakraborty, M. Davis, M. Dustin, M. Kardar, E. Pamer, A. Perelson, D. Portnoy and A. Shaw (members of the program project (AI-071195) under which this work was initiated). Supported by the US National Institutes of Health (AI-24157).

AUTHOR CONTRIBUTIONS

S.P.P., K.S.W. and P.M.A. designed the study; S.P.P., K.S.W., C.R.P. and W.-L.L. did all experiments; S.P.P. and P.M.A. wrote the manuscript; K.S.W. did the initial studies with LLO56 and LLO118 mice; and all authors read, commented on and approved of the manuscript before submission.

COMPETING FINANCIAL INTERESTS

The authors declare no competing financial interests.

1. van der Merwe, P.A. & Davis, S.J. Molecular interactions mediating T cell antigen recognition. *Annu. Rev. Immunol.* **21**, 659–684 (2003).
2. Davis, M.M. *et al.* Ligand recognition by αβ T cell receptors. *Annu. Rev. Immunol.* **16**, 523–544 (1998).
3. Morris, G.P. & Allen, P.M. How the TCR balances sensitivity and specificity for the recognition of self and pathogens. *Nat. Immunol.* **13**, 121–128 (2012).
4. Ernst, B., Lee, D.S., Chang, J.M., Sprent, J. & Surh, C.D. The peptide ligands mediating positive selection in the thymus control T cell survival and homeostatic proliferation in the periphery. *Immunity* **11**, 173–181 (1999).
5. Krogsgaard, M. *et al.* Agonist/endogenous peptide-MHC heterodimers drive T cell activation and sensitivity. *Nature* **434**, 238–243 (2005).
6. Lo, W.L. *et al.* An endogenous peptide positively selects and augments the activation and survival of peripheral CD4$^+$ T cells. *Nat. Immunol.* **10**, 1155–1161 (2009).
7. Kirberg, J., Berns, A. & von Boehmer, H. Peripheral T cell survival requires continual ligation of the T cell receptor to major histocompatibility complex-encoded molecules. *J. Exp. Med.* **186**, 1269–1275 (1997).
8. Cho, J.H., Kim, H.O., Surh, C.D. & Sprent, J. T cell receptor-dependent regulation of lipid rafts controls naive CD8$^+$ T cell homeostasis. *Immunity* **32**, 214–226 (2010).
9. Kersh, G.J. *et al.* Structural and functional consequences of altering a peptide MHC anchor residue. *J. Immunol.* **166**, 3345–3354 (2001).
10. Hataye, J., Moon, J.J., Khoruts, A., Reilly, C. & Jenkins, M.K. Naive and memory CD4$^+$ T cell survival controlled by clonal abundance. *Science* **312**, 114–116 (2006).
11. Obar, J.J., Khanna, K.M. & Lefrancois, L. Endogenous naive CD8$^+$ T cell precursor frequency regulates primary and memory responses to infection. *Immunity* **28**, 859–869 (2008).
12. Malherbe, L., Hausl, C., Teyton, L. & McHeyzer-Williams, M.G. Clonal selection of helper T cells is determined by an affinity threshold with no further skewing of TCR binding properties. *Immunity* **21**, 669–679 (2004).
13. Busch, D.H. & Pamer, E.G. T cell affinity maturation by selective expansion during infection. *J. Exp. Med.* **189**, 701–710 (1999).
14. Moon, J.J. *et al.* Naive CD4$^+$ T cell frequency varies for different epitopes and predicts repertoire diversity and response magnitude. *Immunity* **27**, 203–213 (2007).
15. Zehn, D., Lee, S.Y. & Bevan, M.J. Complete but curtailed T-cell response to very low-affinity antigen. *Nature* **458**, 211–214 (2009).
16. Azzam, H.S. *et al.* CD5 expression is developmentally regulated by T cell receptor (TCR) signals and TCR avidity. *J. Exp. Med.* **188**, 2301–2311 (1998).

17. Mandl, J.N., Monteiro, J.P., Vrisekoop, N. & Germain, R.N. T cell-positive selection uses self-ligand binding strength to optimize repertoire recognition of foreign antigens. *Immunity* **38**, 263–274 (2013).
18. Weber, K.S. *et al.* Distinct CD4+ helper T cells involved in primary and secondary responses to infection. *Proc. Natl. Acad. Sci. USA* **109**, 9511–9516 (2012).
19. Lenardo, M. *et al.* Mature T lymphocyte apoptosis–immune regulation in a dynamic and unpredictable antigenic environment. *Annu. Rev. Immunol.* **17**, 221–253 (1999).
20. Hochweller, K. *et al.* Dendritic cells control T cell tonic signaling required for responsiveness to foreign antigen. *Proc. Natl. Acad. Sci. USA* **107**, 5931–5936 (2010).
21. Stefanová, I., Dorfman, J.R. & Germain, R.N. Self-recognition promotes the foreign antigen sensitivity of naive T lymphocytes. *Nature* **420**, 429–434 (2002).
22. Lo, W.L., Donermeyer, D.L. & Allen, P.M. A voltage-gated sodium channel is essential for the positive selection of CD4+ T cells. *Nat. Immunol.* **13**, 880–887 (2012).
23. Kaye, J., Kersh, G., Engel, I. & Hedrick, S.M. Structure and specificity of the T cell antigen receptor. *Semin. Immunol.* **3**, 269–281 (1991).
24. Moran, A.E. *et al.* T cell receptor signal strength in Treg and iNKT cell development demonstrated by a novel fluorescent reporter mouse. *J. Exp. Med.* **208**, 1279–1289 (2011).
25. Smith, K. *et al.* Sensory adaptation in naive peripheral CD4 T cells. *J. Exp. Med.* **194**, 1253–1261 (2001).
26. Skoberne, M., Holtappels, R., Hof, H. & Geginat, G. Dynamic antigen presentation patterns of Listeria monocytogenes-derived CD8 T cell epitopes in vivo. *J. Immunol.* **167**, 2209–2218 (2001).
27. Tarakhovsky, A. *et al.* A role for CD5 in TCR-mediated signal transduction and thymocyte selection. *Science* **269**, 535–537 (1995).
28. Zhou, X.Y. *et al.* CD5 costimulation up-regulates the signaling to extracellular signal-regulated kinase activation in CD4+CD8+ thymocytes and supports their differentiation to the CD4 lineage. *J. Immunol.* **164**, 1260–1268 (2000).
29. Peña-Rossi, C. *et al.* Negative regulation of CD4 lineage development and responses by CD5. *J. Immunol.* **163**, 6494–6501 (1999).
30. Azzam, H.S. *et al.* Fine tuning of TCR signaling by CD5. *J. Immunol.* **166**, 5464–5472 (2001).
31. Gapin, L., Matsuda, J.L., Surh, C.D. & Kronenberg, M. NKT cells derive from double-positive thymocytes that are positively selected by CD1d. *Nat. Immunol.* **2**, 971–978 (2001).
32. Lio, C.W. & Hsieh, C.S. A two-step process for thymic regulatory T cell development. *Immunity* **28**, 100–111 (2008).
33. Stritesky, G.L., Jameson, S.C. & Hogquist, K.A. Selection of self-reactive T cells in the thymus. *Annu. Rev. Immunol.* **30**, 95–114 (2012).
34. Zikherman, J., Parameswaran, R. & Weiss, A. Endogenous antigen tunes the responsiveness of naive B cells but not T cells. *Nature* **489**, 160–164 (2012).
35. Daniels, M.A. *et al.* Thymic selection threshold defined by compartmentalization of Ras/MAPK signalling. *Nature* **444**, 724–729 (2006).
36. Huang, J. *et al.* The kinetics of two-dimensional TCR and pMHC interactions determine T-cell responsiveness. *Nature* **464**, 932–936 (2010).
37. Sabatino, J.J. Jr., Huang, J., Zhu, C. & Evavold, B.D. High prevalence of low affinity peptide-MHC II tetramer-negative effectors during polyclonal CD4+ T cell responses. *J. Exp. Med.* **208**, 81–90 (2011).
38. Tubo, N.J. *et al.* Single naive CD4+ T cells from a diverse repertoire produce different effector cell types during infection. *Cell* **153**, 785–796 (2013).
39. Kim, C., Wilson, T., Fischer, K.F. & Williams, M.A. Sustained interactions between T cell receptors and antigens promote the differentiation of CD4+ memory T cells. *Immunity* **39**, 508–520 (2013).
40. Martin, B. *et al.* Highly self-reactive naive CD4 T cells are prone to differentiate into regulatory T cells. *Nat. Commun.* **4**, 2209 (2013).

ONLINE METHODS

Mice. LLO56 (B6 Thy-1.1$^+$ *Rag1*$^{-/-}$) mice and LLO118 (B6 Ly5.1$^+$ *Rag1*$^{-/-}$) mice have been described[18]. The CD4$^+$ T cells in LLO56 and LLO118 mice express a single, distinct TCR (α-chain variable region 2 and β-chain variable region 2 ($V_\alpha 2V_\beta 2$)) that recognizes LLO residues 190–205 bound to I-A^b. LLO56 and LLO118 mice were maintained in the heterozygous state for the TCR-encoding transgenes. B6 and MHC class II–deficient mice were from The Jackson Laboratory. CD5-deficient mice were obtained as part of the National Institute of Allergy and Infectious Diseases Exchange Program from the transgenic mouse repository maintained by Taconic. Mice doubly deficient in H-2M and β_2-microglobulin were provided by the laboratory of J. Ting; these mice were backcrossed to B6 mice, and the F_1 progeny were intercrossed to restore the wild-type alleles encoding β_2-microglobulin, thus generating the H-2M-deficient mice used in this study. Mice with transgenic expression of the AND TCR on the *H2*^{k} and *H2*^{b} MHC haplotype backgrounds (AND *Rag1*$^{-/-}$ *H2*^{k} and AND *H2*^{b}, respectively) and mice deficient in the α-chain constant region of the TCR from our colony were also used in some of the experiments here. All mice were between 4 and 12 weeks of age at the beginning of each experiment, with all experimental comparisons done without 'blinding' of researchers to mouse identity for age- and sex-matched cohorts. As they were extensively backcrossed, all age- and sex-matched mice of a given strain were considered to be identical and were assigned randomly to treatment groups. Breeding, housing and care of all mice was done in specific pathogen–free facilities under a protocol approved by the Washington University Animal Studies Committee.

Antibodies and other reagents. The following antibodies were used for flow cytometry: anti-CD4 (RM4-4, RM4-5 and GK1.5), anti-CD8 (53-7.8), anti-CD69 (H1.2F3), anti-CD25 (PC61), anti-IL-2 (JES6-5H4), anti-IFNγ (XMG1.2), anti-TNF (MP6-XT22), anti-CD28 (37.51), anti-CD3ε(145-2C11), anti–Vα2TCR (B20.1), anti–γδ TCR (GL3), anti-CD44 (IM7), anti-CD127 (SB/199) and anti-I-A^b (KH74; all from Biolegend); anti-CD5 (53-7.3; BD Biosciences and Biolegend); anti-B220 (RA3-6B2; eBioscience and Biolegend); anti-F4/80 (BM8; Invitrogen and Biolegend); anti-CD11b (M1/70; eBioscience and BD Biosciences); anti-CD11c (N418; Biolegend), anti-PD-1 (J43), anti-PD-L1 (MIH5), anti-CTLA-4 (UC10-4F10-11) and anti-Bcl-2 (3F11; all from BD Biosciences); anti-Thy-1.1 (HIS51) and anti-Ly5.1 (A20; both from Biolegend and eBioscience); and anti-NK1.1 (PK136; eBioscience). Rabbit antibody to phosphorylated Erk1/2 (also used for immunoblot analysis; D13.14.4E) and rabbit antibody to phosphorylated Bim (C34C5), rabbit IgG isotype-matched control antibody (DA1E), and Alexa Fluor 647–conjugated anti-rabbit IgG F(ab′)$_2$ (4414) were from Cell Signaling Technologies. Annexin V was from BD Biosciences, and 7-AAD (7-amino-actinomycin D) was from Sigma-Aldrich.

The following primary antibodies were used for immunoblot analysis: antibody to phosphorylated tyrosine (4G10; Upstate Biotechnology), anti-IκBα (9242; Cell Signaling) and anti-β-actin (2F1-1; Biolegend). Polyclonal rabbit anti-TCRζ serum 777, which recognizes unphosphorylated and phosphorylated TCRζ, was generated in our laboratory as described[41]. Secondary antibodies used for detection in immunoblots included Alexa Fluor 680–conjugated goat anti–rabbit IgG (A21109; Molecular Probes) and IRDye 800CW–conjugated anti–mouse IgG (926-32210; LI-COR).

Analysis of T cell activation. For analysis of the upregulation of the expression of activation markers, enzyme-linked immunosorbent assays and cytokine capture assays, LLO56 and LLO118 CD4$^+$ T cells purified by magnetic bead negative selection were cultured with T cell–depleted B6 splenocyte samples at a ratio of 1:4. Cells were stimulated in duplicate or triplicate wells at 37 °C in 5% CO_2 in DMEM plus 10% FCS (HyClone). The mouse cytokine-capture assay was done according to the manufacturer's protocol (Miltenyi Biotec), except that the culture medium contained bovine serum rather than mouse serum. For this assay, anti-CD3ε (145-2C11; Biolegend) and anti-CD28 (37.51; Biolegend) were used for stimulation; PMA (phorbol 12-myristate 13-acetate) and ionomycin was not used with this assay to avoid cytokine capture in *trans* by nonsecreting cells.

Intracellular cytokine staining was done as described[15]. Cells were incubated for 30 min with 100 ng/ml PMA (Sigma-Aldrich) plus 1 μg/ml ionomycin (Sigma-Aldrich), then incubated for an additional 4 h with 2 μg/ml brefeldin A (Sigma-Aldrich). Samples were harvested and then stained for surface markers with anti-CD4 (GK1.5; Biolegend), anti-CD8 (53-7.8; Biolegend), anti-CD5 (53-7.3; BD Biosciences), anti-Thy-1.1 (HIS51; eBioscience) and/or anti-Ly5.1 (A20; eBioscience) and with 7-AAD, then were fixed in 4% paraformaldehyde in PBS and permeabilized in flow cytometry buffer containing 0.5% saponin (Sigma-Aldrich), then were stained with anti-IL-2 (JES6-5H4; Biolegend), anti-IFNγ (XMG1.2; Biolegend) and anti-TNF (MP6-XT22; Biolegend).

Surface plasmon resonance. A Biacore 2000 SPR system was used for binding experiments essentially as described[42]. CM5 sensor chips (GE Healthcare) were activated by a 20-minute pulse of a 1:1 mixture of NHS (*N*-hydroxysuccinimide) and EDC (1-ethyl-3-[3-dimethylaminopropyl] carbodiimide HCl). Soluble LLO(190–205)–I-A^b was amine-coupled to the chip in 20 mM sodium citrate, pH 4.5, to a total response of 300 response units, after which unreacted NHS groups on the chip were blocked by a 6-minute pulse of 1 M ethanolamine, pH 8.5. A series of concentrations of soluble LLO56 and LLO118 single-chain TCRs in HEPES-buffered saline and BSA (10 mM HEPES, 3 mM EDTA, 150 mM NaCl, 0.05% Tween-20 and 1% BSA) were injected in duplicate over prepared flow cells at a flow rate of 30 μl/min. Specific surface plasmon resonance responses of the binding of the TCRs to LLO(190–205)–I-A^b were obtained by subtraction of the response obtained by injection over a flow cell coupled with unexchanged soluble I-A^b, followed by correction for bulk flow effects by subtraction of the response obtained by injection of plain buffer. Sensorgrams were fitted by BiaEvaluation software to a 1:1 Langmuir binding model to derive values for the dissociation rate constant k_d and association rate constant k_a and the dissociation constant K_d (k_d/k_a).

Preparation of soluble protein. Soluble LLO56 and LLO118 single-chain TCRs, designed as V_β-linker-V_α constructs, were engineered by error-prone mutagenesis and conformational selection of stable mutants by yeast display as described[43]. The genes encoding single-chain TCRs were cloned into plasmid pET28a at NheI-XhoI restriction sites, which placed them in-frame with a six-histidine tag. Protein expression in *Escherichia coli* was induced with 1 mM IPTG (isopropyl β-D-thiogalactopyranoside) and thus generated insoluble single-chain TCR inclusion bodies that were harvested as described[44]. Inclusion bodies were then refolded under oxidative conditions and purified by nickel bead batch purification (Qiagen), followed by size-exclusion chromatography with an S200 FPLC. Purified proteins were concentrated with Amicon centrifugal filters and were quantified by their absorbance of ultraviolet radiation at 280 nm with extinction coefficients of 1.690 and 1.674 for LLO56 single-chain TCRs and LLO118 single-chain TCRs, respectively. For the preparation of LLO(190–205)–I-A^b complexes, soluble 3R–I-A^b (I-A^b covalently tethered to 3R, an arginine-substituted variant of the peptide derived from the MHC class II molecule I-E^a, amino acids 52–68) was provided by E. Huseby. 3R–I-A^b complexes were engineered with a thrombin site in the linker connecting the I-A^b molecule to the peptide, which allowed the peptide to be released by treatment with thrombin. Following overnight cleavage with thrombin at room temperature, 3R peptide bound to I-A^b was exchanged with LLO(190–205) by incubation for 48 h at 37 °C in sodium carbonate buffer, pH 10.5.

Flow cytometry analysis of phosphorylated Erk. Cells were prepared in triplicate in a volume of 100 μl in serum-free IMDM and were stored on ice before activation. After the addition of 100 μl PMA at 2× concentration (200 ng/ml), each tube was briefly mixed, then placed in a 37 °C water bath to begin the stimulation. Afterward, tubes were removed from the water bath and immediately fixed by the addition of 200 μl of 4% paraformaldehyde in PBS. After 20 min of fixation at room temperature, tubes were filled with 4 ml ice-cold 100% methanol and stored overnight at 4 °C. The next day, cells were washed twice, incubated with rabbit antibody to phosphorylated Erk [(identified above), then stained with Alexa Fluor 647–conjugated antibody to rabbit IgG F(ab′)$_2$ (4414; Cell Signaling) along with anti-CD4 (GK1.5; Biolegend), anti-CD8 (53-7.8; Biolegend), anti-CD5 (53-7.3; BD Biosciences), anti-Thy-1.1 (HIS51; eBioscience) and/or anti-Ly5.1 (A20; eBioscience).

Immunoblot analysis. Cells were stimulated at 37 °C, then lysed immediately in ice-cold buffer containing 1% Nonidet P-40, leupeptin and pepstatin A (10 μg/ml each), 1 mM PMSF and 1 mM sodium orthovanadate. Lysates were cleared of insoluble material by centrifugation at 16,000*g* for 10 min at 4 °C, then were mixed with Laemmli buffer, boiled for 5 min and separated by 12% SDS-PAGE. After overnight transfer to nitrocellulose membranes (10 V and 4 °C), nonspecific binding was blocked for 1 h with a 1:1 mixture of PBS and Odyssey Blocking Buffer (LI-COR), followed by incubation overnight at 4 °C with mouse and rabbit primary antibodies (identified above), and then incubation with the secondary antibodies Alexa Fluor 680–conjugated goat anti–rabbit IgG (A21109; Molecular Probes) and IRDye 800CW–conjugated goat anti–mouse IgG (926-32210; LI-COR). All antibody incubation steps were done in a 1:1 mixture of PBS and Odyssey Blocking Buffer with 0.1% Tween-20. Membranes were imaged with an Odyssey infrared scanner (LI-COR), and densitometry was assessed with ImageJ software (NIH).

Analysis of Ca^{2+} flux. T cells purified by magnetic sorting were stained for 30 min at 37 °C with 2 μM Indo-1 AM (Molecular Probes) in the presence of 0.02% Pluronic-F127. Cells were washed twice, resuspended in buffered saline containing 1 mM $CaCl_2$ and 1 mM $MgCl_2$ and allowed to 'rest' for 20–30 min at room temperature. All samples were prewarmed to 37 °C for 5 min immediately before analysis. After a baseline was established with unstimulated cells, ionomycin was added to a final concentration of 5 μg/ml.

Flow cytometry and cell sorting. A BD FACSCalibur or BD LSR II was used for flow cytometry. For cell sorting, single-cell suspensions of thymus or pooled spleen and lymph nodes were stained for populations of interest with anti-CD4, anti-CD8 and anti-CD5 (identified above). For sorting of B6 T cells by CD5 expression, samples were pre-enriched for $CD4^+$ or $CD8^+$ T cells by magnetic sorting. $CD44^{hi}$, $CD25^+$ and $NK1.1^+$ were removed as part of our sorting strategy in some experiments to generate populations of naive conventional $CD4^+$ or $CD8^+$ T cells. Samples were routinely costained with 7-AAD and anti-CD11b, anti-CD11c, anti-B220 and anti-F4/80 (identified above) to facilitate exclusion of dead and unwanted cells. A FACSAria II sorter (BD Biosciences) was used for all cell sorting. Data for all these experiments were analyzed with FlowJo software, version 8.8.6 (Treestar).

Expression of human VGSC in peripheral $CD4^+$ T cells. The human SCN5A–green fluorescent protein construct was a gift from K. Murray[45]. The cDNA encoding human SCN4B (RC223951; Origene) was amplified by PCR and cloned into plasmid pcDNA3.1. Peripheral $CD4^+$ T cells were isolated by magnetic sorting and were transfected by electroporation with constructs encoding SCN5A–green fluorescent protein and SCN4B-mCherry (with the Amaxa Nucleofector kit for primary mouse T cells). Cells were then allowed to 'rest' for 3 h, cultured overnight with irradiated B6 APCs and analyzed by flow cytometry for upregulation of CD69 expression with anti-CD69 (H1.2F3; Biolegend). All experiments used viable $VGSC^+$ $CD4^+$ T cells, defined as cells successfully transfected with both plasmids (positive for green fluorescent protein and mCherry). For MHC class II–blocking studies, APCs were preincubated with 10 μg/ml anti $I\text{-}A^b$ (KH74; Biolegend) at least 15 min before the addition of transfected T cells.

Adoptive-transfer experiments. LLO56 and LLO118 $CD4^+$ T cells were purified by magnetic bead negative selection. LLO56 and LLO118 $CD4^+$ T cells (1×10^6 to 3×10^6) were transferred intravenously into B6 recipients, MHC Class II–deficient recipients, recipients deficient in the α-chain constant region of the TCR, or H-2M–deficient recipients for 1, 2 or 4 or 6 d, depending on the experiment, then were harvested and subjected to magnetic enrichment as described[46]. For experiments in which IL-2 production was assayed in donor cells, enrichment was routinely done by positive selection for their unique congenic markers, with similar results if cells underwent enrichment by negative selection. For experiments in which phosphorylated Erk was assayed in donor cells or donor cells were transferred into *L. monocytogenes*–infected mice, cells were purified exclusively by negative selection. In experiments where donor cells were purified then transferred into *L. monocytogenes*–infected mice, 3×10^3 purified donor cells (LLO56 or LLO118 T cells, either initially deprived or not deprived of MHC class II) were transferred.

Labeling with the cytosolic dye CFSE. Purified LLO56 and LLO118 T cells were stained with CFSE (carboxyfluorescein diacetate-succinimidyl ester; Molecular Probes) at a final concentration of 5 μM, then were washed three times in PBS plus 0.1% BSA, then counted and used immediately in adoptive transfer experiments.

Infection with *L. monocytogenes*. Frozen stocks of *L. monocytogenes* strain 10403S in PBS plus 20% glycerol were thawed and serially diluted to a density of 1×10^4 colony-forming units per ml in PBS; 100 μL of that solution was injected retro-orbitally to produce an inoculum of 1×10^3 colony-forming units per mouse. Injection titers were confirmed by counting colonies in aliquots of injection solution plated on brain-heart–infusion agar.

Statistic analysis. Statistical tests are indicated in figure legends. A P value of <0.05 was designated as the criterion for significance. Decisions to use the statistical test noted were assisted by the results of the Shapiro-Wilk normality test and the F test (to compare variances). Sample size determination was not done to choose the sizes of experimental groups in this study. Prism 6 for Mac OS X (GraphPad) was used for all statistical analysis.

41. Kersh, E.N., Shaw, A.S. & Allen, P.M. Fidelity of T cell activation through multistep T cell receptor zeta phosphorylation. *Science* **281**, 572–575 (1998).
42. Persaud, S.P., Donermeyer, D.L., Weber, K.S., Kranz, D.M. & Allen, P.M. High-affinity T cell receptor differentiates cognate peptide-MHC and altered peptide ligands with distinct kinetics and thermodynamics. *Mol. Immunol.* **47**, 1793–1801 (2010).
43. Weber, K.S., Donermeyer, D.L., Allen, P.M. & Kranz, D.M. Class II-restricted T cell receptor engineered *in vitro* for higher affinity retains peptide specificity and function. *Proc. Natl. Acad. Sci. USA* **102**, 19033–19038 (2005).
44. Garcia, K.C., Radu, C.G., Ho, J., Ober, R.J. & Ward, E.S. Kinetics and thermodynamics of T cell receptor- autoantigen interactions in murine experimental autoimmune encephalomyelitis. *Proc. Natl. Acad. Sci. USA* **98**, 6818–6823 (2001).
45. Hallaq, H. *et al.* Activation of protein kinase C alters the intracellular distribution and mobility of cardiac Na^+ channels. *Am. J. Physiol. Heart Circ. Physiol.* **302**, H782–H789 (2012).
46. Moon, J.J. *et al.* Tracking epitope-specific T cells. *Nat. Protoc.* **4**, 565–581 (2009).

doi:10.1038/ni.2822